J. Fluid Mech. (1971), *vol.* 46, *part* 3, *pp.* 521–544
Printed in Great Britain

Hydromechanics of swimming propulsion. Part 2. Some optimum shape problems

By T. YAO-TSU WU

California Institute of Technology
Pasadena, California

(Received 21 July 1970)

The optimum shape problems considered in this part are for those profiles of a two-dimensional flexible plate in time-harmonic motion that will minimize the energy loss under the condition of fixed thrust and possibly also under other isoperimetric constraints. First, the optimum movement of a rigid plate is completely determined; it is necessary first to reduce the original singular quadratic form representing the energy loss to a regular one of a lower order, which is then tractable by usual variational methods. A favourable range of the reduced frequency is found in which the thrust contribution coming from the leading-edge suction is as small as possible under the prescribed conditions, outside of which this contribution becomes so large as to be hard to realize in practice without stalling. This optimum solution is compared with the recent theory of Lighthill (1970); these independently arrived-at conclusions are found to be virtually in agreement.

The present theory is further applied to predict the movement of a porpoise tail of large aspect-ratio and is found in satisfactory agreement with the experimental measurements. A qualitative discussion of the wing movement in flapping flight of birds is also given on the basis of optimum efficiency.

The optimum shape of a flexible plate is analysed for the most general case of infinite degrees of freedom. It is shown that the solution can be determined to a certain extent, but the exact shape is not always uniquely determinate.

1. Introduction

One of the most inspiring questions concerning the phenomena of aquatic animal propulsion and of flapping flights of birds and insects is invariably connected with the highest possible hydrodynamic efficiency. This problem has been brought up from time to time by various observers who have noted the impressive capabilitity of these animals in generating fast movements at low energy cost. According to the first principle of energy balance or momentum consideration, as has been explained in part 1 of this paper (Wu 1971), much can already be said about the desirable shapes of body movement: that at large Reynolds numbers, a thin two-dimensional plate gains thrust by sending a transverse wave from head to tail, with amplitude slightly increasing towards the rear, thereby achieving a forward swimming velocity somewhat less than the phase velocity of the body wave form. As for the tail of large aspect-ratio

of some high-performance fish, the tail should move nearly tangentially to the path traversed in the space by the body wave form. These basic features have been elegantly elucidated, with perhaps more physical reasoning, in an excellent review by Lighthill (1969). However, it would still be of great interest to resolve a quantitative determination of the optimum shape under some appropriate constraints.

The problem of the optimum shape is interesting in its own right from the mathematical point of view, since the effective methods of solution do not seem to fall into the known categories of the calculus of variation. The special case of a two-dimensional waving plate in harmonic motion has been treated by Wang (1966), who adopted a discretized Fourier representation of the body motion, and found that his solutions exist only for a set of eigenvalues. However, it is found in the present study that this optimum shape problem is basically not an eigenvalue problem, and therefore merits a new discussion. On physical grounds, it would be indeed difficult to see the significance of the idea that the shape function can have eigensolutions.

In this part we shall consider the optimum shape problem only for the case of two-dimensional flexible plate, of negligible thickness, in harmonic motion. (Some three-dimensional problems will be treated in part 3 of this paper.) The two-dimensional theory is reckoned to have utility in problems of lifting surfaces of large aspect-ratio, such as the tails of some cetaceans and high-performance game fish (the lunate tails: swordfish, tuna, albacore, porpoises, etc.), and even the wings of most birds and some insects. The optimum shape problem is concerned with those profiles or movements that will minimize the energy loss under the condition of fixed thrust (required to overcome the viscous drag), and possibly also under other isoperimetric constraints. First, the optimum movement of a rigid plate is determined by reducing the original singular problem to a regular one of a lower rank. This optimum solution is found to depend on two variables: one being the reduced frequency and the other a 'proportional-loading parameter', defined as the prescribed thrust coefficient divided by the dimensionless heaving amplitude squared. For given loading parameter, a favourable range of the reduced frequency is found in which the thrust contribution coming from the leading edge suction is as small as possible under the prescribed conditions. This consideration seems to provide the optimum range of the reduced frequency utilized in practice.

These theoretical results are further applied to predict the movement of a porpoise tail, and comparisons made with the experimental investigation of Lang & Daybell (1963). As a related problem of interest, the optimum movement of a flapping wing of some birds or flatfish is discussed qualitatively.

The general problem of optimum shape of a flexible surface having an infinite degree of freedom is finally analysed and discussed. It is found that the solution can be determined to a certain extent, and, with the additional degrees of freedom, the optimum efficiency can be further improved from the rigid-plate value, but the exact shape is not uniquely determinate.

2. Statement of the optimum shape problem

As a starting point, the following basic results are reproduced from part 1 (Wu 1971). The class of motion treated here is that of a two-dimensional flexible plate, immersed parallel to a uniform stream of velocity U in the x-direction, and performing a harmonic transverse motion

$$y = h(x,t) = h_1(x)\exp(j\omega t) \quad (-1 \leqslant x \leqslant 1), \tag{1}$$

which is assumed to be continuous in $-1 \leqslant x \leqslant 1$ and to possess a Fourier expansion

$$h(x,t) = \tfrac{1}{2}\beta_0 + \sum_{n=1}^{N} \beta_n \cos n\theta \quad (x = \cos\theta,\ 0 \leqslant \theta \leqslant \pi), \tag{2}$$

with

$$\beta_n = \frac{2}{\pi}\int_0^{\pi} h(x,t)\cos n\theta\, d\theta \quad (n = 0,\ 1 \ldots N \leqslant \infty).$$

This motion generates at the plate a transverse flow velocity,

$$V(x,t) = \frac{\partial h}{\partial t} + U\frac{\partial h}{\partial x} = U\left(\frac{\partial h}{\partial x} + j\sigma h\right) \quad (\sigma = \omega/U), \tag{3}$$

which can also be expanded in a Fourier series,

$$V(x,t) = \tfrac{1}{2}b_0 + \sum_{n=1}^{N} b_n \cos n\theta \quad (x = \cos\theta), \tag{4}$$

with

$$b_n = \frac{2}{\pi}\int_0^{\pi} V(x,t)\cos n\theta\, d\theta \quad (n = 0,\ 1 \ldots N \leqslant \infty).$$

In (2)–(4) and in the sequel, the harmonic time factor $\exp(j\omega t)$ of h, V, β_n's and b_n's is always taken as understood. The reduced frequency σ is referred to half-chord l, which is being taken as the unit length, or

$$\sigma = \omega l/U. \tag{5}$$

The time averages of thrust $\bar{T}$, energy loss $\bar{E}$, and power required $\bar{P}$ can be put in the coefficient form,

$$C_E \equiv \bar{E}/(\tfrac{1}{4}\pi\rho U^3 l) = B(\sigma)(b_0 + b_1)(b_0^* + b_1^*)/U^2, \tag{6}$$

$$C_P \equiv \bar{P}/(\tfrac{1}{4}\pi\rho U^3 l) = \mathrm{Re}\{-(j\sigma/U)(b_0 + b_1)[(\beta_0^* - \beta_1^*)\Theta(\sigma) + \beta_1^*]\}, \tag{7}$$

$$C_T \equiv \bar{T}/(\tfrac{1}{4}\pi\rho U^2 l) = C_P - C_E, \tag{8}$$

where the symbols with * stand for their complex conjugates, $\Theta(\sigma)$ denotes Theodorsen's function

$$\Theta(\sigma) = K_1(j\sigma)/[K_0(j\sigma) + K_1(j\sigma)] = \mathscr{F} + j\mathscr{G}, \tag{9a}$$

$$B(\sigma) = \mathscr{F} - (\mathscr{F}^2 + \mathscr{G}^2), \tag{9b}$$

K_n being the modified Bessel function of the second kind, $\mathscr{F}$ and $\mathscr{G}$ being the real and imaginary parts of Θ.

The general optimum shape problem can be stated as follows: Within the class of shape function h as specified above, find the optimum one which will minimize C_E under the condition of fixed thrust coefficient, say

$$C_T = C_{T,0} > 0, \tag{10}$$

the reduced frequency being regarded as a fixed parameter.

As has been pointed out in part 1, $C_E \geqslant 0$ for $\sigma > 0$ with any admissible h, consequently the extremal solution of C_E will not be negative. Here, C_T rather than C_p is chosen to be a fixed positive quantity for the sole reason that the result will always give a meaningful hydrodynamic efficiency:

$$\eta = C_T/C_p = C_{T,0}/C_p = C_{T,0}/(C_{T,0}+C_E). \tag{11}$$

If C_p is fixed instead, the solution of C_T may become negative. Aside from this point, there is no fundamental difference whether C_T or C_p is fixed.

It is of interest to note that only the first two Fourier coefficients of h and of V appear in the expressions for C_E, C_P and C_T. Since h and V are related by a differential equation (3), b_n can be expressed in terms of β_n's upon substituting (2), (4) in (3). Conversely, if V is first prescribed by a set of b_n's, β_n can be evaluated in terms of b_n upon integration of (3), thus introducing a complementary solution proportional to $\exp(-j\sigma x)$. In either case, b_0 and b_1 will depend on all the β_n's which are admitted to h, or β_0 and β_1 will depend on all the b_n's admitted to V. If the number N of the terms in (2), (4), is taken to be infinite, so that h and V each will define a vector space of infinite dimensions, the problem can be recast somewhat as follows. Define the scalar product of two functions $h(x)$ and $g(x)$ over $-1 \leqslant x \leqslant 1$ by

$$(h,g) = \frac{2}{\pi}\int_0^\pi h(x)\,g^*(x)\,d\theta \quad (x = \cos\theta), \tag{12}$$

then (6), (7) may be written

$$C_E = U^{-2}B(\sigma)(V, 1+x)(V^*, 1+x), \tag{13}$$

$$C_P = \mathrm{Re}\{(-j\sigma/U)(V, 1+x)[(h^*, 1)\,\Theta(\sigma) + (h^*, x)(1-\Theta(\sigma))]\}. \tag{14}$$

A striking feature here is that there are only three different scalar products involving h and V that can be subjected to variation, from which the optimum h is to be determined.

The number of the Fourier coefficients, or equivalently, the number of scalar products can be increased by a few if the waving plate propels itself without external agencies whilst the recoil conditions are imposed on the plate's being free from lateral and angular recoil. These recoil conditions require that the hydrodynamic lift L and moment M must be equal and opposite to the time-rate of change of the lateral and angular momentum of the body (see (40), (41), (56) of part 1), or

$$(b_0+b_1)\,\Theta(\sigma) + \tfrac{1}{2}j\sigma(b_0-b_2) = +\frac{U\sigma^2}{\pi\rho}\int_{-1}^{1} m(x)\,h(x)\,dx, \tag{15}$$

$$(b_0+b_1)\,\Theta(\sigma) - (b_1+b_2) - \tfrac{1}{4}j\sigma(b_1-b_3) = -\frac{2U\sigma^2}{\pi\rho}\int_{-1}^{1} xm(x)\,h(x)\,dx, \tag{16}$$

where $m(x)$ is the plate mass per unit distance in x. Conditions (15), (16) are additional isoperimetric conditions to be satisfied together with (10) in extremizing C_E. These two conditions can, however, be disregarded or accounted for separately, when this two-dimensional theory is applied to evaluate the propulsion of a lifting surface (of large aspect-ratio) which is only a part of the self-

propelling body, such as the tail of certain cetaceans and Lunate tails, or the wings of birds, since the question of recoil requires a consideration of the entire body.

3. Optimum movement of a rigid-plate wing

The basic nature of this optimum shape problem can be best seen from the following simple case:

$$h(x,t) = [\tfrac{1}{2}\xi_0 + (\xi_1 + j\xi_2)\,x]\exp(j\omega t) \quad (|x| \leqslant 1), \tag{17a}$$

so that

$$\beta_0 = \xi_0 \exp(j\omega t), \quad \beta_1 = (\xi_1 + j\xi_2)\exp(j\omega t), \tag{17b}$$

where ξ_0, ξ_1, ξ_2 are real. The above h represents a rigid plate performing a heaving with amplitude $\frac{1}{2}\xi_0$ and a pitching about $x = 0$ with amplitude $|\xi_1 + j\xi_2|$ at a phase angle $\tan^{-1}(\xi_2/\xi_1)$ leading the heaving motion. This special case, though about the simplest in form for the general optimum problem, still embraces a considerable interest for its result may cast light on the tail motion of some high-performance fish and cetacean, as well as on the flapping wings of birds in flight.

Before we proceed further, we list here two fundamental cases:

(i) *Heaving* only, so that $\xi_1 = \xi_2 = 0$ and only $\xi_0 \neq 0$. Then, by (2)–(4),

$$b_0 = Uj\sigma\xi_0 \exp(j\omega t), \quad b_1 = 0. \tag{18}$$

The corresponding C_T, C_E, C_P are

$$C_E = \sigma^2 B(\sigma)\,\xi_0^2, \quad C_P = \sigma^2 \mathscr{F}(\sigma)\,\xi_0^2, \quad C_T = \sigma^2(\mathscr{F}^2 + \mathscr{G}^2)\,\xi_0^2. \tag{19}$$

The hydrodynamic efficiency of heaving propulsion,

$$\eta_{\text{heav}}(\sigma) = C_T/C_P = (\mathscr{F}^2 + \mathscr{G}^2)/\mathscr{F}, \tag{20}$$

is seen to depend on σ only, decreasing monotonically from $\eta_h(0) = 1$ to $\eta_h(\infty) = 0{\cdot}5$, as shown in figure 1. This general trend of η_h is readily verified from the known asymptotic behaviour of $\mathscr{F}$ and $\mathscr{G}$ that, for $\sigma \ll 1$,

$$\mathscr{F}(\sigma) \sim 1 - \frac{\pi\sigma}{2} - \sigma^2\left(\log^2\frac{2}{\gamma_1\sigma} - \frac{\pi^2}{4}\right) + O(\sigma^3\log^2\sigma) \quad (\gamma_1 = 1{\cdot}781\ldots), \tag{21a}$$

$$\mathscr{G}(\sigma) \sim -\sigma(1 - \pi\sigma)\log\frac{2}{\gamma_1\sigma} + O(\sigma^3\log^3\sigma), \tag{21b}$$

and, for $\sigma \gg 1$,

$$\mathscr{F}(\sigma) \sim \frac{1}{2}\left[1 + \frac{1}{8\sigma^2} + O(\sigma^{-4})\right], \quad \mathscr{G}(\sigma) \sim -\frac{1}{8\sigma}\left[1 - \frac{11}{128\sigma^2} + O(\sigma^{-4})\right]. \tag{22}$$

(ii) *Pitching* only, so that $\xi_0 = 0$ and we may also set $\xi_2 = 0$ as a reference phase,

$$\beta_0 = 0, \quad \beta_1 = \xi_1, \quad b_0 = 2U\xi_1, \quad b_1 = Uj\sigma\xi_1, \tag{23}$$

in which the harmonic time factors are omitted as understood. Whence, from (6)–(8),

$$C_E = B(\sigma)\,Q_{22}\xi_1^2, \quad C_P = \sigma P_{22}\xi_1^2, \quad C_T = T_{22}\xi_1^2, \tag{24}$$

where

$$Q_{22} = 4 + \sigma^2, \quad P_{22} = \sigma(1 - \mathscr{F}) - 2\mathscr{G}, \quad T_{22} = \sigma P_{22} - BQ_{22}. \tag{25}$$

In this pure-pitching mode, both C_E and C_P are positive definite for $\sigma > 0$. But $T_{22}(\sigma) = 0$ has one real root,

$$T_{22}(\sigma_0) = 0 \quad \text{for} \quad \sigma_0 = 1{\cdot}781, \tag{26}$$

and $T_{22} \lesseqgtr 0$ according as $\sigma \lesseqgtr \sigma_0$ (see figure 2 for its numerical value). When $C_T > 0$, we may define the hydrodynamic efficiency

$$\eta_{\text{pitch}}(\sigma) = \frac{C_T}{C_P} = \frac{T_{22}(\sigma)}{\sigma P_{22}(\sigma)} \quad (\sigma > \sigma_0), \tag{27}$$

which is found to increase monotonically from $\eta_p(\sigma_0) = 0$ to $\eta_p(\infty) = 0{\cdot}5$, as shown in figure 1. We further note that in either case (i) or (ii), power must be

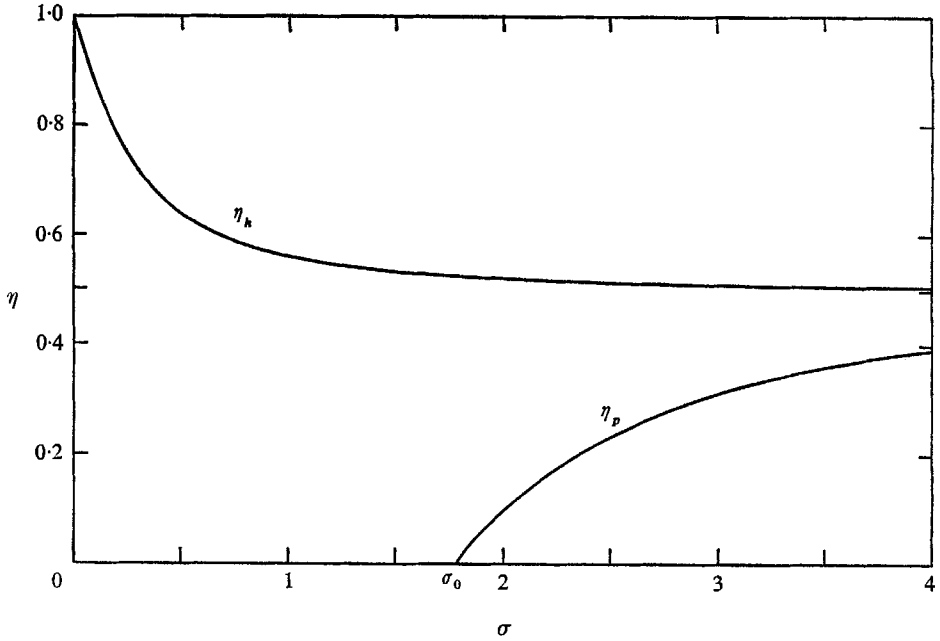

FIGURE 1. Hydrodynamic efficiency of heaving propulsion, $\eta_h(\sigma)$, and of pitching propulsion, $\eta_p(\sigma)$, the latter being defined for the reduced frequency $\sigma > \sigma_0 = 1{\cdot}781$.

supplied to maintain the motion, consequently it is impossible to extract energy from the fluid in so far as either (i) or (ii) is concerned separately. The main objective of optimization is then to determine if the efficiency can be greatly improved when both heaving and pitching modes are admitted.

Returning to the combined motion, the value of $(b_0 + b_1)$ corresponding to h of (17) is, by (3) and (4),

$$b_0 + b_1 = U \exp(j\omega t)\,[j\sigma\xi_0 + (2 + j\sigma)(\xi_1 + j\xi_2)]. \tag{28}$$

We note here that $b_0 + b_1 = 0$ when

$$\xi_1 = \hat{\xi}_1 \equiv -\sigma^2(\sigma^2+4)^{-1}\xi_0, \quad \xi_2 = \hat{\xi}_2 \equiv -2\sigma(\sigma^2+4)^{-1}\xi_0. \tag{29}$$

At the same time, C_E, C_P and C_T all vanish with $(b_0 + b_1)$, according to (6)–(8). This particular set of values $(\xi_0, \hat{\xi}_1, \hat{\xi}_2)$ will be seen to play a significant role in the

optimum solution. Upon substituting (17), (28) in (6) and (7), C_E and C_P can be written

$$C_E = B(\sigma)(\boldsymbol{\xi}, \mathbf{Q}\boldsymbol{\xi}), \quad C_P = \sigma(\boldsymbol{\xi}, \mathbf{P}\boldsymbol{\xi}) \tag{30}$$

where $\boldsymbol{\xi} = (\xi_0, \xi_1, \xi_2)$ is a vector in a 3-dimensional vector space, $(\boldsymbol{\xi}, \boldsymbol{\zeta})$ denotes the inner product of $\boldsymbol{\xi}$ and $\boldsymbol{\zeta}$, or $\xi_0\zeta_0+\xi_1\zeta_1+\xi_2\zeta_2$, $\mathbf{Q}$ and $\mathbf{P}$ are 3×3 symmetric matrices with elements,

$$\left.\begin{aligned} &Q_{11} = Q_{12} = \sigma^2, \quad Q_{13} = 2\sigma, \quad Q_{22} = Q_{33} = 4+\sigma^2, \quad Q_{23} = 0; \\ &P_{11} = \sigma\mathscr{F}, \quad P_{12} = \mathscr{G}+\tfrac{1}{2}\sigma, \quad P_{13} = \mathscr{F}-\sigma\mathscr{G}, \quad P_{22} = P_{33} = \sigma(1-\mathscr{F})-2\mathscr{G}, \\ &\qquad\qquad\qquad\qquad\qquad\qquad\qquad\qquad\qquad\qquad P_{23} = 0. \end{aligned}\right\} \tag{31}$$

Q_{22} and P_{22} in (31) are identical to (25). It can be shown from the properties of $\mathscr{F}$ and $\mathscr{G}$ that $\mathbf{P}$ is non-singular for $\sigma > 0$ since none of the three eigenvalues of $\mathbf{P}$ vanishes for $\sigma > 0$. However, $\mathbf{Q}$ has the eigenvalues 0, (σ^2+4), $(2\sigma^2+4)$, and hence $\mathbf{Q}$ is singular in the third order, but non-singular in the second order.

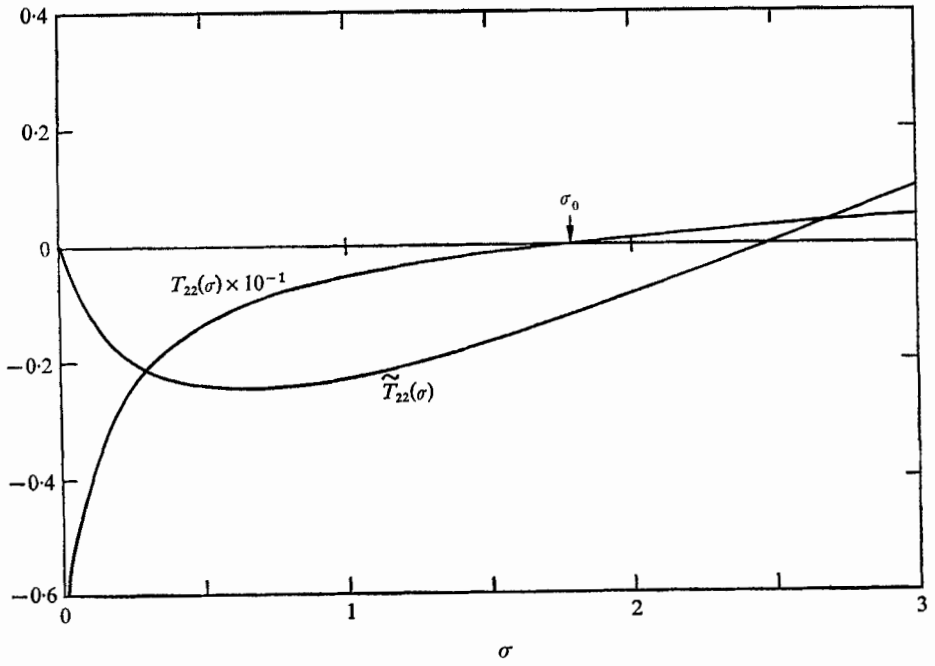

FIGURE 2. Coefficient $T_{22}(\sigma)$ associated with pitching of a rigid plate and $\tilde{T}_{22}(\sigma)$ pertaining to a flexible plate.

The optimum problem at hand is to minimize the quadratic form C_E of (30) under the constraint (10), whereas the recoil conditions (15), (16) are relaxed for the reason already stated. This constrained optimization is equivalent to minimizing a new function,

$$C'_E = C_E - \lambda'(C_T - C_{T,0}) = (1+\lambda')C_E - \lambda' C_P + \lambda' C_{T,0}, \tag{32}$$

λ' being a Lagrange multiplier. If one sets all the derivatives of C'_E with respect to ξ_0, ξ_1, ξ_2 to zero, one finds that the secular equation,

$$|\mathbf{Q}-\mu\mathbf{P}| = 0 \text{ has three roots: } \mu_1 = 0, \mu_2 = 0, \mu_3 = Q_{22}/P_{22}, \tag{33}$$

where μ is related to the old multiplier λ' (the actual relationship being immaterial). The first two eigenvalues μ_1, μ_2, being a double root of zero, yield the same eigenvector $(\xi_0, \hat{\xi}_1, \hat{\xi}_2)$ with $\hat{\xi}_1, \hat{\xi}_2$ given by (29). But, as noted before, $b_0+b_1=0$ when $\xi_1=\hat{\xi}_1$, $\xi_2=\hat{\xi}_2$, thereby making C_E, C_P and C_T all vanish. Clearly this eigenvector is not the solution since condition (10) can not be satisfied. (The generalized eigenvector of rank 2 in the sense $\mathbf{Q}^2\boldsymbol{\xi}=0$, $\mathbf{Q}\boldsymbol{\xi}\neq 0$ for the multiple root μ_2 does not exist, nor does any generalized eigenvector of higher ranks.) The third eigenvalue μ_3 gives the eigenvector having $\xi_0=0$; the resulting C_E therefore becomes proportional to C_T, implying that this last eigenvector is a stationary solution. This also shows that the foregoing method based on the spectral theory, as was used by Wang (1966), does not work.

The correct approach is found by noting that since $\mathbf{Q}$ is singular, but non-singular in the second order, the quadratic form C_E can always be reduced to a non-singular form in two variables. In fact, in terms of the new variables,

$$\zeta_0=\xi_0/(4+\sigma^2), \quad \zeta_1=\xi_1-\hat{\xi}_1, \quad \zeta_2=\xi_2-\hat{\xi}_2, \tag{34}$$

with $\hat{\xi}_1, \hat{\xi}_2$ given by (29), C_E and C_P in (30) reduce to

$$C_E=B(\sigma)\,Q_{22}(\zeta_1^2+\zeta_2^2), \tag{35}$$

$$C_P=\sigma\{P_{22}(\zeta_1^2+\zeta_2^2)+2A_1\zeta_0\zeta_1+2A_2\zeta_0\zeta_2\}, \tag{36}$$

$$A_1=P_{12}Q_{22}-Q_{12}P_{22}, \quad A_2=P_{13}Q_{33}-Q_{13}P_{33}. \tag{37}$$

Now it is clear that, while C_P spans the whole vector space $(\zeta_0, \zeta_1, \zeta_2)$, C_E spans only its subspace (ζ_1, ζ_2). Obviously the surface $C_E=\text{const.}=C_{E,0}>0$ is a circular cylinder with its central axis along the ζ_0-axis. The quadric $C_P=\text{const.}=C_{P,0}>0$ is seen to be an oblique hyperboloid of one sheet, since its intersection with the plane $\zeta_0=\text{const.}$ is a circle centred at $(-A_1\zeta_0/P_{22}, -A_2\zeta_0/P_{22})$, of radius $[(A_1^2+A_2^2)(\zeta_0/P_{22})^2+C_P/(\sigma P_{22})]^{\frac{1}{2}}$. The extremal solutions under condition (10) are therefore given by the points in the subspace (ζ_1, ζ_2) at which (grad C_E) is proportional to (grad C_P). This situation is depicted in figure 3 in terms of C_E and C_T. Thus, after setting the derivatives of $C_E'=(C_E-\lambda'' C_P)$ with respect to ζ_1 and ζ_2 to zero, we obtain

$$\zeta_1=\lambda A_1\zeta_0, \quad \zeta_2=\lambda A_2\zeta_0 \tag{38}$$

where λ is a Lagrange multiplier. Upon substituting (38) in (35)–(36),

$$C_E=BQ_{22}\lambda^2(A\zeta_0)^2, \quad A^2=A_1^2+A_2^2, \tag{39}$$

$$C_P=\sigma(P_{22}\lambda^2+2\lambda)(A\zeta_0)^2. \tag{40}$$

Now, application of condition (10), or $C_P-C_E=C_{T,0}$, results in a quadratic equation for λ,

$$T_{22}(\sigma)\lambda^2+2\sigma\lambda=\bar{C}_{T,0}(4+\sigma^2)^2/A^2, \tag{41a}$$

where

$$\bar{C}_{T,0}=C_{T,0}/\xi_0^2, \quad A^2=A_1^2+A_2^2, \tag{41b}$$

and $T_{22}(\sigma)$ is given by (25). $\bar{C}_{T,0}$ will be called the 'proportional-loading parameter'. The multiplier λ therefore has two solutions

$$\left.\begin{matrix}\lambda_1\\ \lambda_2\end{matrix}\right\}=\frac{\sigma}{T_{22}}\{-1\pm(1+\Lambda)^{\frac{1}{2}}\}, \quad \Lambda=\bar{C}_{T,0}T_{22}\left(\frac{\sigma^2+4}{\sigma A}\right)^2. \tag{42}$$

λ_1, λ_2 depend on two parameters: σ and $\bar{C}_{T,0}$. By virtue of the behaviour $T_{22}(\sigma) \gtrless 0$ according as $\sigma \gtrless \sigma_0 = 1{\cdot}781$, it follows that for fixed $\bar{C}_{T,0} > 0$, $\Lambda(\sigma, \bar{C}_{T,0})$ increases monotonically from $-\infty$ to 0 as σ moves from $\sigma = 0$ to σ_0. Consequently, λ_1, λ_2 will be real (as are required to be physically meaningful) if $\Lambda \geqslant -1$; or, equivalently, for

$$\sigma \geqslant \sigma_c(\bar{C}_{T,0}), \quad \text{where} \quad \Lambda(\sigma_c, \bar{C}_{T,0}) = -1. \tag{43}$$

The solution $\sigma_c = \sigma_c(\bar{C}_{T,0})$ is shown in figure 4 to lie between $\sigma_c(0) = 0$ and $\sigma_c(\infty) = \sigma_0$. For given $\bar{C}_{T,0} > 0$, the real optimum solution therefore exists only

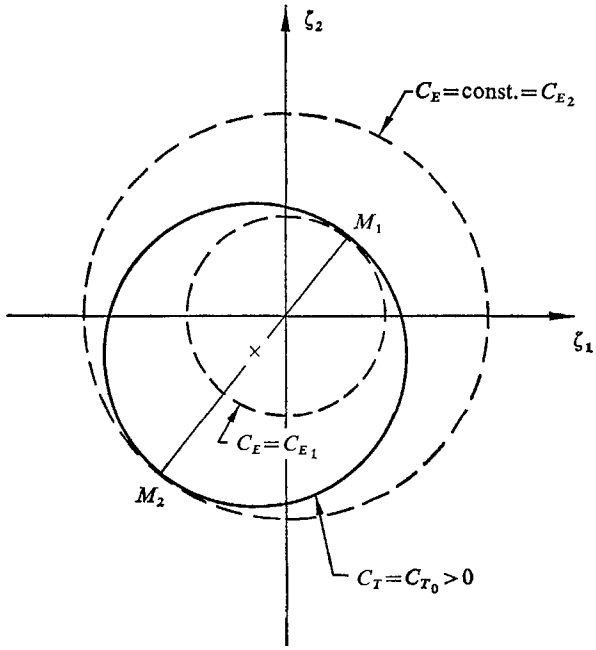

FIGURE 3. For ζ_0 fixed, the quadric $C_T = C_{T,0} > 0$ is an off-centred circle which meets tangentially the surface $C_E = C_{E,1}$ at M_1 and $C_E = C_{E,2}$ ($> C_{E,1}$) at M_2. The points M_1 and M_2 correspond, respectively, the maximum and minimum hydrodynamic efficiency under condition of fixed $C_T = C_{T,0}$.

for $\sigma \geqslant \sigma_c$. Within this range, λ_1 is positive, numerically smaller than λ_2, and corresponds to the highest efficiency attainable under condition (10),

$$\eta_{\max} = \frac{C_{T,0}}{C_P} = 1 - \frac{C_E}{C_P} = 1 - \frac{BQ_{22}\lambda_1}{\sigma(P_{22}\lambda_1 + 2)} \quad (\sigma \geqslant \sigma_c). \tag{44}$$

The lowest efficiency $\eta_{\min}$ that can be realized under the same conditions (10) is given by the last expression of (44) with λ_1 replaced by λ_2. For any combination of ζ_0, ζ_1, ζ_2 different from (38), the efficiency η is $\eta_{\min} < \eta < \eta_{\max}$ so long as $\bar{C}_{T,0}$ is kept fixed.

The following salient features of the solution are noteworthy.

(i) At $\sigma = \sigma_c$, $\Lambda = -1$, so that $\lambda_1 = \lambda_2 = -\sigma_c/T_{22}(\sigma_c)$; hence, from (44) and (25), it follows that for arbitrary $\bar{C}_{T,0} > 0$

$$\eta_{\max}(\sigma_c) = [2 + P_{22}(\sigma_c)\lambda_1(\sigma_c)]^{-1} < \tfrac{1}{2} \tag{45}$$

in virtue of $P_{22}(\sigma) > 0$ and $\lambda_1(\sigma_c) > 0$. This shows that, in the frequency range near σ_c, $\eta_{\max}$ cannot be very impressive. In fact, $\eta_{\max}(\sigma_c) \to 0$ monotonically as $\bar{C}_{T,0} \to \infty$, since in this limit $T_{22}(\sigma_c) \to T_{22}(\sigma_0) = 0$, and hence $\lambda_1 \to \infty$ (see figure 4).

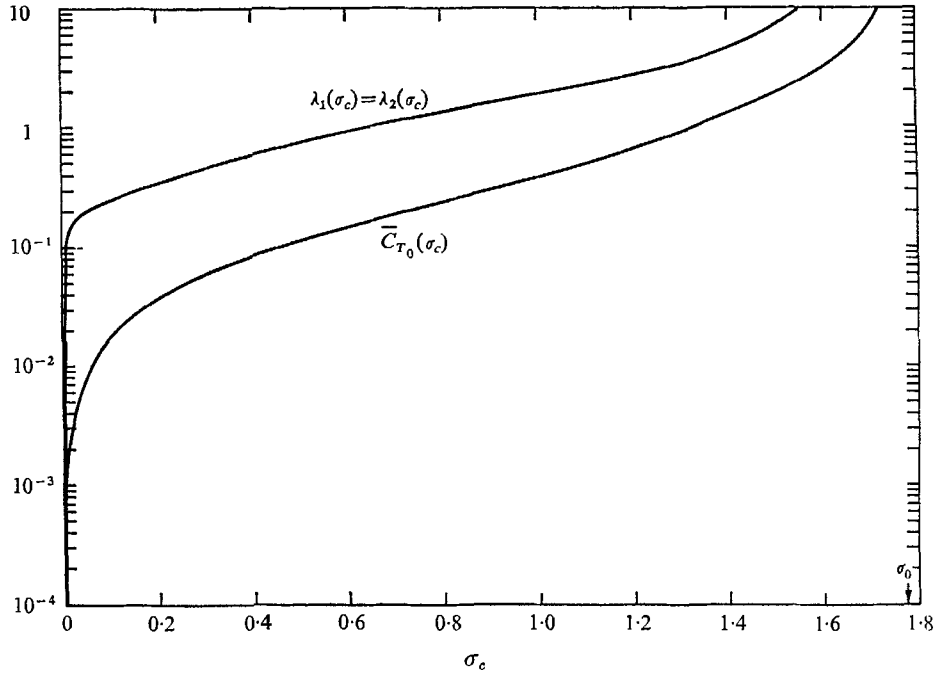

FIGURE 4. For given $\bar{C}_{T,0} > 0$, the critical σ_c marks the lower bound of the reduced frequency σ, below which no real optimum solution exists.

However, when $\bar{C}_{T,0} \ll 1$, σ_c is also small. By making use of the asymptotic expansions (21) for $\mathscr{F}$ and $\mathscr{G}$, we readily deduce that

$$\sigma_c \sim 2\pi\bar{C}_{T,0}\left\{1+\bar{C}_{T,0}\left[\left(2-\frac{1}{\pi}\right)\log\frac{2}{\gamma_1\bar{C}_{T,0}}+\frac{\pi}{2}\right]+O(\sigma_c^2\log^2\sigma_c)\right\}, \tag{46}$$

$$\eta_{\max} \sim \frac{1}{2}\left\{1-\frac{\sigma}{2\pi}\log\frac{2}{\gamma_1\sigma}+\left(\frac{\sigma-\sigma_c}{\sigma}\right)^{\frac{1}{2}}\left[1-\frac{\pi+4}{4}\sigma\log\frac{2}{\gamma_1\sigma}\right]\right\}, \tag{47}$$

the last expression being valid for $0 \leqslant (\sigma-\sigma_c) \ll 1$. Note that $d\eta(\sigma_c)/d\sigma = \infty$; thus $\eta_{\max}$ rises rapidly from $\eta_{\max}(\sigma_c)$ as σ increases from σ_c.

(ii) Near $\sigma = \sigma_0$ (σ_0 defined by (26)), we deduce from (26), (44), and (22) that

$$\lambda_1(\sigma) = \tfrac{1}{2}\bar{C}_{T,0}(\sigma_0^2+4)^2/(\sigma_0 A^2)+O(|\sigma-\sigma_0|), \tag{48}$$

$$\eta_{\max}(\sigma) = [1+\tfrac{1}{2}P_{22}(\sigma_0)\lambda_1(\sigma_0)]^{-1}+O(|\sigma-\sigma_0|) \simeq [1+\tfrac{8}{9}\bar{C}_{T,0}]^{-1}+O(|\sigma-\sigma_0|). \tag{49}$$

We note that $\eta_{\max}(\sigma_0)$ is already more than twice $\eta_{\max}(\sigma_c)$.

(iii) For $\bar{C}_{T,0} \ll 1$ and $\sigma_c \ll \sigma$, Λ is small, say $\Lambda = \epsilon \ll 1$. Then $\lambda_1 = O(\epsilon)$, consequently $\eta_{\max} = 1-O(\epsilon)$ for $\sigma_c \ll \sigma$, indicating that high efficiencies can be achieved in the neighbourhood of $\bar{C}_{T,0} = C_{T,0}/\xi_0^2 = 0$. In this operating region the amplitude of heaving of course must not vanish ($\xi_0 \neq 0$). In the limit as $\bar{C}_{T,0} \to 0$, $\lambda_1 \to 0$, and hence ζ_1, ζ_2 $\bar{T}$, $\bar{E}$, $\bar{P}$ all tend to zero whereas $\eta_{\max} \to 1$, corresponding to the singular case already mentioned in part 1.

(iv) For $\sigma \gg 1$, we deduce from (44), by using expansions (22), that, for arbitrary $\bar{C}_{T,0} > 0$,

$$\eta_{\max} \sim \left[1+\tfrac{4}{9}\bar{C}_{T,0}\left(1-\frac{15}{4\sigma^2}\right)\right]\left[1+\tfrac{8}{9}\bar{C}_{T,0}\left(1-\frac{5}{24\sigma^2}\right)\right]^{-1}, \tag{50}$$

which has the bounds $0{\cdot}5 < \eta_{\max} < 1$. The lower bound corresponds to large $\bar{C}_{T,0}$, a limit which is reached as the flapping amplitude $\xi_0 \to 0$. This result is in

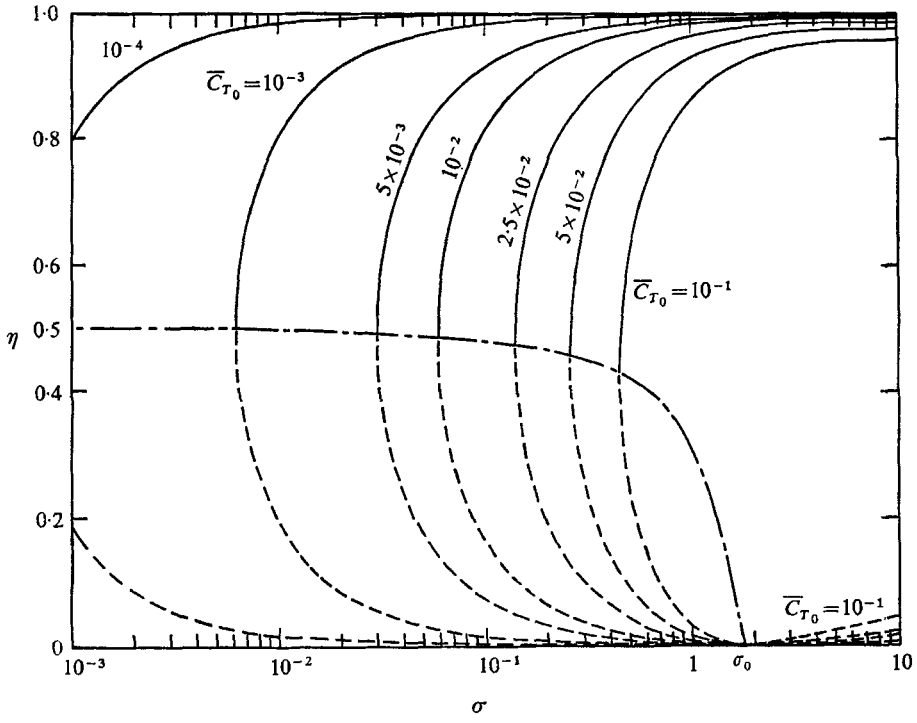

FIGURE 5. Maximum and minimum efficiencies for fixed $\bar{C}_{T,0}$:
———, $\eta_{\max}$; – – – –, $\eta_{\min}$; — — —, $\eta_{\max}(\sigma_c, \bar{C}_{T,0})$.

accordance with the special case of pure pitching oscillation (see (27) and figure 1), namely, it can be used to produce thrust only when σ is sufficiently high, at the expense of low efficiency.

The above features are all exhibited in the numerical result of $\eta_{\max}$ as plotted in figure 5 for several values of $\bar{C}_{T,0}$.

The optimum motion of the plate is given by (34), (38), (29) and (42),

$$\xi_1/\xi_0 = (\lambda_1 A_1 - \sigma^2)/(\sigma^2+4), \quad \xi_2/\xi_0 = (\lambda_1 A_2 - 2\sigma)/(\sigma^2+4). \tag{51}$$

Hence, the amplitude ratio and the phase advance of pitching relative to the heaving mode are

$$Z_p \equiv (\xi_1^2+\xi_2^2)^{\frac{1}{2}}/\xi_0 = (\sigma^2+4)^{-1}[(\lambda_1 A_1-\sigma^2)^2+(\lambda_1 A_2-2\sigma)^2]^{\frac{1}{2}}. \tag{52a}$$

$$\alpha_p = \tan^{-1}\xi_2/\xi_1 = \tan^{-1}[(\lambda_1 A_2-2\sigma)/(\lambda_1 A_1-\sigma^2)]. \tag{52b}$$

These results are shown in figures 6 and 7 for several values of $\bar{C}_{T,0}$. For σ sufficiently large, say $\sigma > 2$, curves of different $\bar{C}_{T,0}(< 1)$ approach to a common asymptotic representation:

$$Z_p \sim \frac{\sigma^2 + 2(1 - 5\bar{C}_{T,0}/3)}{\sigma^2 + 4}, \quad \alpha_p \sim \pi + \tan^{-1}\left[\frac{2}{\sigma}\left(1 + \tfrac{2}{3}\bar{C}_{T,0}\right)\right]. \tag{53}$$

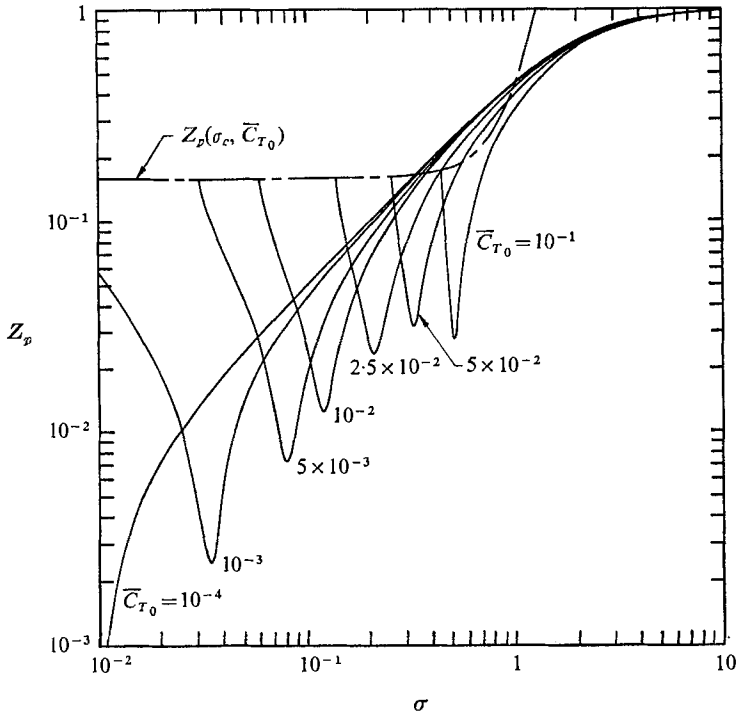

FIGURE 6. The amplitude ratio (pitching/heaving) $Z_p(\sigma, \bar{C}_{T,0})$.

In summary, we first notice the advantage of operating at small values of $\bar{C}_{T,0}$, corresponding to sufficiently large heaving amplitude. A smaller $\bar{C}_{T,0}$ renders the optimum solution valid to lower frequencies σ, and makes $\eta_{\max}$ greater at the same σ. As σ increases from σ_c, the pitching-heaving amplitude ratio Z_p first decreases to a minimum, then increases steadily to a common asymptote. Over the same range of σ, the phase difference α_p changes very rapidly at first, followed by a much slower variation at higher σ. A rather sophisticated control would therefore be necessary if the operating range of σ is chosen in which fast variations of Z_p and α_p may take place. It is a remarkable result that in the higher range of σ, very high efficiencies can be realized with an appropriate interplay between the heaving and pitching motions. This effect is exhibited in the result with the pitching amplitude as little as only a small fraction ($\sim$ 0·1 or less) of the heaving motion, provided the phase difference is correctly observed.

The foregoing exposition of the optimum solution leaves very little clue as to whether there also exists an optimum range of σ (aside from the understanding

that σ should be sufficiently greater than σ_c) for practical operations. A possible source for such crucial information lies in the knowledge of the thrust contribution coming from the leading-edge suction, as was pointed out by Lighthill (1970), for the following reason. Although this suction force has been simplified to appear mathematically as a singular force acting on a pointed leading edge, it can be realized physically only when the thin section's leading edge is sufficiently rounded. The magnitude of this suction is therefore of utmost importance to its being realizable or not in practice.

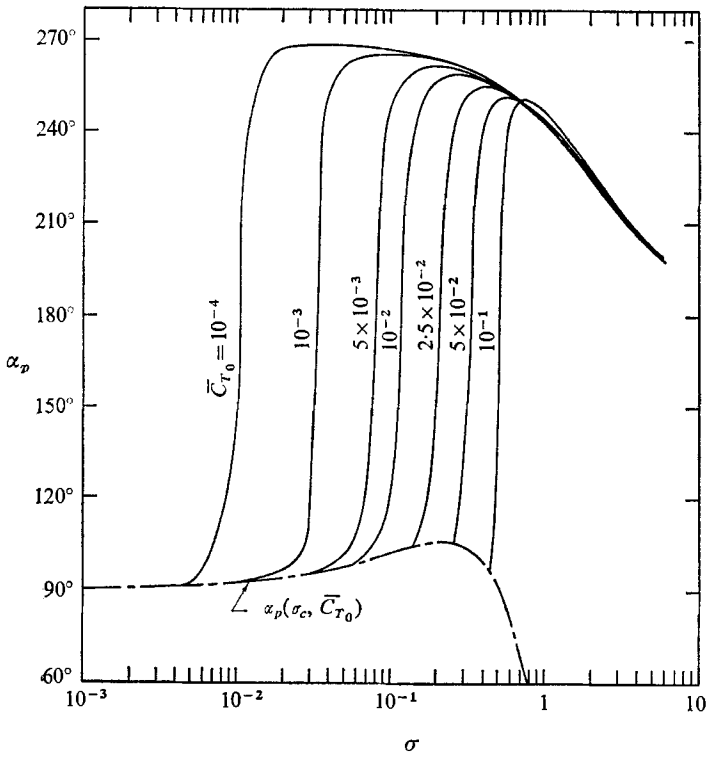

FIGURE 7. The phase advance angle $\alpha_p(\sigma, \bar{C}_{T,0})$ of the pitching mode.

The leading-edge suction is given by (see part 1, equations (43), (62))

$$T_S = \tfrac{1}{8}\pi\rho(a_0+a_0^*)^2, \quad a_0 = (b_0+b_1)\,\Theta(\sigma)-b_1.$$

Its time average in harmonic motions is clearly

$$\bar{T}_S = \tfrac{1}{4}\pi\rho a_0 a_0^*, \tag{54}$$

which can be expressed in terms of ξ_0, ξ_1, ξ_2 for the motion given by (17) by a straightforward substitution upon using (9a), (28), yielding for the ratio of the mean suction thrust coefficient $C_S \equiv \bar{T}_S/(\frac{1}{4}\pi\rho U^2 l)$, to the prescribed total thrust coefficient $C_T = C_{T,0}$ as

$$C_S/C_T = (\bar{C}_{T,0})^{-1}\left\{\left[(\sigma\mathscr{G}-2\mathscr{F})\frac{\xi_1}{\xi_0}-P_{22}\frac{\xi_2}{\xi_0}+\sigma\mathscr{G}\right]^2 + \left[(\sigma\mathscr{G}-2\mathscr{F})\frac{\xi_2}{\xi_0}+P_{22}\frac{\xi_1}{\xi_0}-\sigma\mathscr{F}\right]^2\right\}. \tag{55}$$

For the optimum movement, ξ_1/ξ_0 and ξ_2/ξ_0 in (55) assume the values given by (51). The final result is plotted in figure 8 for various proportional-loading parameter $\bar{C}_{T,0}$. It is of great interest to note that the ratio C_S/C_T has a minimum at $\sigma = \sigma_m(\bar{C}_{T,0})$ say, and is relatively small in a short stretch of σ about σ_m. Outside of this range, C_S/C_T increases rapidly beyond 1 and becomes so large (the complementary thrust delivered by the plate surface is then negative) as to be certainly difficult to realize in practice without leading-edge stalling. It is also noteworthy that $\sigma = \sigma_m$ is very near the corresponding maximum of the $\alpha_p(\sigma)$ curve about which α_p varies relatively slowly with σ. It is thus convincing that the optimum range of operating σ in practice should be somewhere very near σ_m, most likely to be a little greater than σ_m before C_S/C_T rises sharply so that a slightly improved efficiency can be achieved without risking to cause stall.

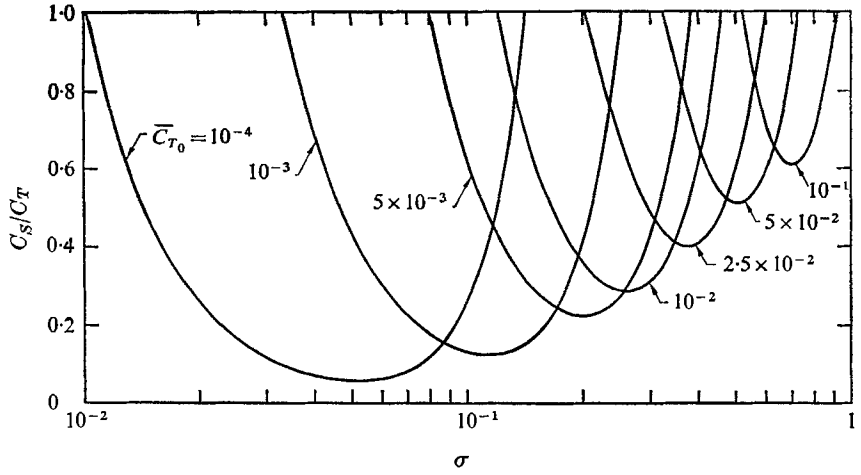

FIGURE 8. The ratio of the thrust coefficient C_S due to leading-edge suction to the total thrust coefficient C_T.

The general problem of optimum movement of a rigid plate was investigated by Lighthill (1970); this study was known to the author when the present paper was written. It is thought to be of interest to discuss these independently arrived-at conclusions. Lighthill takes the section's lateral displacement in the form

$$y = [h - i\alpha(x-b)] \exp(i\omega t) \quad (-l < x < l), \tag{56}$$

where h and α are real numbers signifying the amplitude of the heaving and pitching motions respectively, and $x = b$, $y = 0$ is the axis of pitch. Clearly, Lighthill's adopting a fixed phase difference of 90°, while generalizing the axis of pitch, is equivalent to adopting a general phase difference between heaving and pitching-about-mid-chord-axis. In fact, this equivalence is completed by introducing a reference phase γ to (17), and recovering the half-chord length l,

$$y = [\tfrac{1}{2}l\xi_0 + (\xi_1 + i\xi_2)x] \exp[i(\omega t + \gamma)] \quad (-l < x < l).$$

Then the above two expressions of y are equivalent if

$$b/l = -\tfrac{1}{2}\xi_0\xi_1(\xi_1^2+\xi_2^2)^{-1} = -\tfrac{1}{2}Z_p^{-1}\cos\alpha_p, \tag{57}$$

$$h/l = -\tfrac{1}{2}\xi_0\xi_2(\xi_1^2+\xi_2^2)^{-\frac{1}{2}} = -\tfrac{1}{2}\xi_0\sin\alpha_p, \tag{58}$$

$$\alpha = (\xi_1^2+\xi_2^2)^{\frac{1}{2}} = \xi_0 Z_p. \tag{59}$$

As a useful measure of the relative magnitudes of pitching and heaving, Lighthill (1969, 1970) introduced a 'proportional-feathering parameter', $\theta = U\alpha/\omega h$, which is found to be indicative of thrust and efficiency considerations. Physically, this parameter provides a measure of the deviation of the plate slope from the tangent to the path traversed in the space by the axis of pitch. Since this path is sinusoidal, the largest value α can assume for positive thrust is the maximum slope of the path, $\alpha = kh$, k being the wave-number, which gives

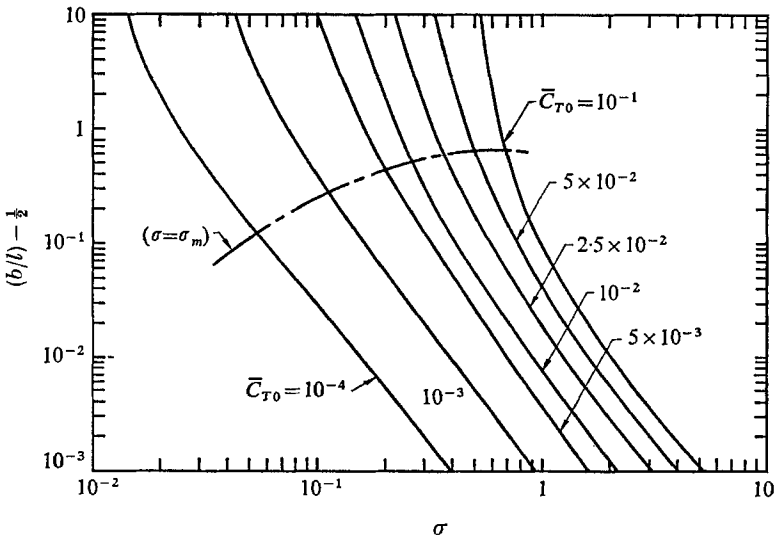

FIGURE 9. The optimum location of pitching axis $x = b$ when the heaving is taken to lead the pitching by 90° in phase. The dotted chain line denotes $\sigma = \sigma_m$ along which the leading-edge suction is minimum.

$\theta = Uk/\omega = U/c$, where c is the wave velocity relative to the plate. Thus, θ is usually less than 1, and $\theta = 1$ corresponds to geometrically accurate feathering of the fin. In terms of the present notation, θ can also be written as

$$\theta \equiv \frac{U\alpha}{\omega h} = -\frac{2}{\sigma}(\xi_1^2+\xi_2^2)/\xi_0\xi_2 = -\frac{2}{\sigma}Z_p\csc\alpha_p. \tag{60}$$

The advantage of Lighthill's form (56) first appears in the result that the wasted energy in the wake has a sharp minimum when $b = \frac{1}{2}l$, or when the pitching axis is at the $\frac{3}{4}$-chord point, whereas the rate of working increases somewhat for axis positions b distal to that. Consequently, an optimum from thrust considerations as well as from efficiency considerations lies somewhere between $b = \frac{1}{2}l$ and $b = l$ (i.e. for the pitching axis to lie between the $\frac{3}{4}$-chord point and the trailing edge).

The present optimization, however, is held under an extra isoperimetric

condition (10) for fixed thrust. The corresponding results of the optimum values of b/l and θ for given $\bar{C}_{T,0}$, by using (51) in (57) and (60), are plotted in figures 9, 10, in which the dotted chain lines correspond to $\sigma = \sigma_m$, along which the leading-edge suction is the smallest possible. Along this line, the pitch-axis b increases from $\frac{1}{2}l$ to $\frac{3}{2}l$ whereas the feathering parameter θ falls off from 1 to 0 as $\bar{C}_{T,0}$ increases. These general features are in qualitative agreement with the

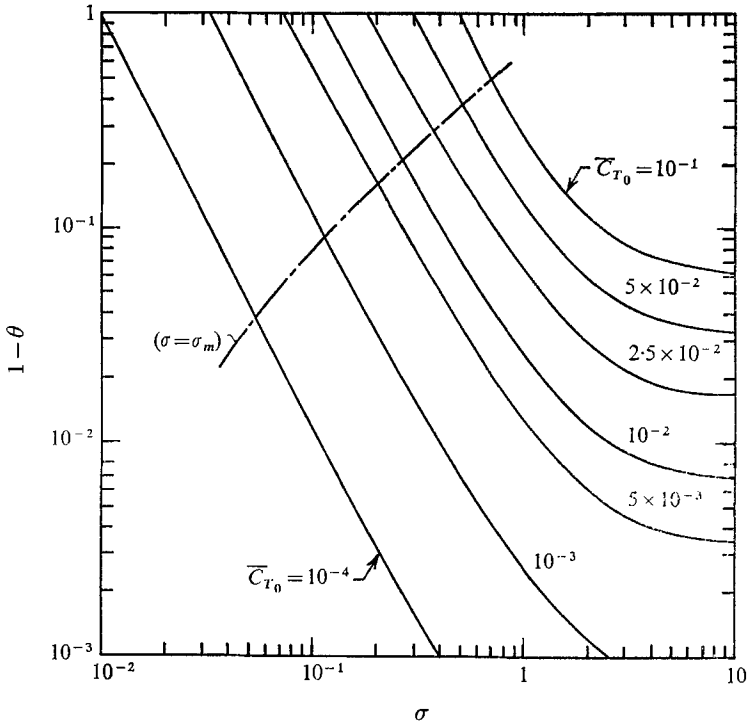

FIGURE 10. Variation of the feathering parameter θ (defined by (60)) with the reduced frequency σ. The dotted chain line denotes $\sigma = \sigma_m$ along which the leading-edge suction is minimum.

predictions of Lighthill (1970). As a further remark here, we note that the point $b/l = \frac{1}{2}$, $\theta = 1$ is readily seen, by (29), (57) and (60), to be equivalent to $\xi_1 = \hat{\xi}_1$, $\xi_2 = \hat{\xi}_2$, of which the significance has already been discussed.

For further comparison of the theory with experiments we proceed to discuss the following specific numerical example.

4. Movements of porpoise tail

Lang & Daybell (1963) reported a series of experiments dealing with the swimming performance of a porpoise (of genus *Lagenorhyncus obliquidens*, or the Pacific Whitesided Dolphin) who was trained to swim and glide along an almost straight course in a long towing tank. This was perhaps one of the very few exhaustive and carefully conducted tests of a live cetacean under a well-controlled condition. The following data, which are thought to be useful for a qualitative comparison, are cited from Lang & Daybell (1963).

The porpoise, 6·7 ft. long, had a total body surface of $S = 16{\cdot}8$ ft^2, including the tail surface area 0·527 ft^2. The tail, nearly triangular but slightly crescent in shape, had a span of 1·69 ft. and a maximum central chord of 0·625 ft., corresponding to an aspect-ratio of 5·4. The total drag D was estimated for full laminar, full turbulent, and 40% laminar flows at various porpoise speeds based on known test data for rigid, smooth ellipsoidal bodies. A particular run selected for the present study was a stretch at porpoise speed $U = 17$ ft./sec, even though a slight acceleration was also recorded. The drag coefficient $C_D = D/(\frac{1}{2}\rho U^2 S)$ equal to 0·0027 based on 40% laminar flow at this speed (or the laminar region Reynolds number of $4{\cdot}2 \times 10^6$) seems to agree fairly well with the observed drag derived from the deceleration measurement during glide runs, though the data of the latter kind have a considerable scatter. This value of C_D will be taken as a representative case for comparison. The amplitude of tail stroke, as measured from this particular run (run no. 15–22, see figure 11) was about 10 in., or 0·83 ft. The tail angles of attack, measured relative to the undulating path traversed by the tail base, are also shown in figure 11 as given by Lang, who remarked on the considerable difficulty of determining the accuracy of the data. As thought to be most likely, the large size of the tail, its great vertical movement, and its noticeable changes in angle of attack would all suggest that a major part (perhaps more than 50%) of the total thrust was produced by the tail alone, leaving the remainder to be generated by the body movement.

Since the aspect-ratio of the tail is sufficiently large to justify the strip theory, we shall adopt this approach, using the local two-dimensional characteristics for each strip. Just as a qualitative estimate we shall further simplify the strip integration by using its algebraic mean, though this will over-estimate the thrust and efficiency. Assuming the total drag D is balanced by the tail thrust during the cruising period, we find

$$C_{T,0} = D/(\tfrac{1}{4}\pi\rho U^2 \tfrac{1}{2} S_{\text{tail}}) = (4/\pi)(S/S_{\text{tail}})C_D = 40{\cdot}5\,C_D = 0{\cdot}11, \tag{61}$$

where C_T stands for the local two-dimensional characteristic. The amplitude of tail stroke of 0·83 ft., when referred to an effective mean half-chord of the tail, $l = 0{\cdot}2$ ft. (which is taken to be slightly on the larger side in order to account for the missing part of the body contribution to the thrust) gives in dimensionless form:

$$\xi_0/2 = (0{\cdot}83)/(0{\cdot}2), \quad \text{or} \quad \xi_0 = 8{\cdot}3,$$

and hence

$$\bar{C}_{T,0} = C_{T,0}/\xi_0^2 = 1{\cdot}6 \times 10^{-3}. \tag{62}$$

The corresponding value of σ_c, by (46), is about $\sigma_c \simeq 0{\cdot}01$. The wavelength of the track of the tail base is estimated from figure 11 to be about $\lambda = 5{\cdot}5$ ft., corresponding to the reduced frequency of the tail motion,

$$\sigma = \frac{\omega l}{U} = \frac{2\pi l}{\lambda} \sim 0{\cdot}4\pi/5{\cdot}5 = 0{\cdot}228, \tag{63}$$

which is very large compared with σ_c, but is quite close to σ_m for this $\bar{C}_{T,0}$.

Now, suppose this tail movement was performed at the optimum efficiency. Then, the efficiency, the amplitude ratio Z_p, and the phase advance α_p of the

pitching mode of the tail are found from figures 6, 7 at the above $\bar{C}_{T,0}$ and σ to be

$$\eta = 0{\cdot}99, \quad Z_p = (\xi_1^2+\xi_2^2)^{\frac{1}{2}}/\xi_0 = 0{\cdot}104, \quad \alpha_p = \tan^{-1}\xi_2/\xi_1 = 263°. \tag{64}$$

The tail motion, upon taking the real part, is

$$h = \tfrac{1}{2}\xi_0 \cos\omega t + (\xi_1 \cos\omega t - \xi_2 \sin\omega t)\, x \quad (-1 < x < 1),$$

where h and x are both referred to the mean half-chord $l = 0{\cdot}2$ ft. The tail angles of attack relative to the free stream is

$$-\partial h/\partial x = -\xi_0 Z_p \cos(\omega t + \alpha_p) = -0{\cdot}862 \cos(\omega t + 263°).$$

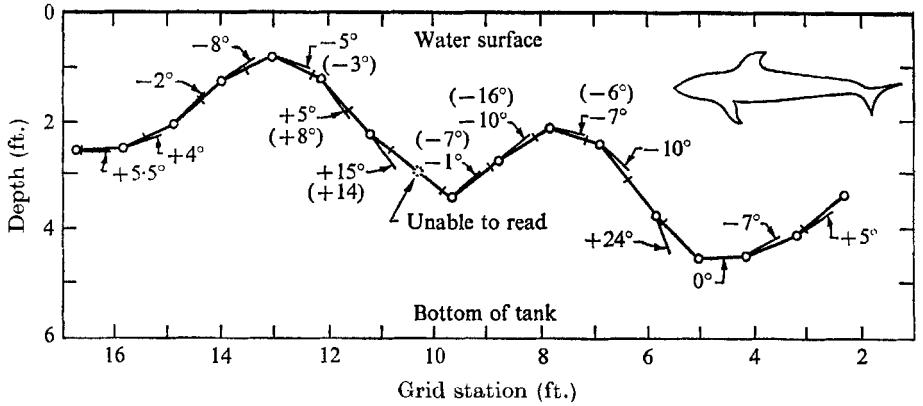

FIGURE 11. Tail movements of a porpoise in cruising. The angles with arrows are the incidence angles of the tail relative to the path of tail-base measured by Lang & Daybell (1963); the angles in parentheses are the present theoretical prediction at the corresponding positions. (Experimental data – –, courtesy of Dr T. G. Lang.)

The slope of the path traversed by the tail base was observed, quite approximately, as $dy/dx = 0{\cdot}55 \sin\omega t$. Hence, the tail angles of attack relative to the path traversed by the tail base is

$$\alpha_{\text{tail}} = dy/dx - \partial h/\partial x \simeq 0{\cdot}55 \sin\omega t - 0{\cdot}862 \sin(\omega t - 7°). \tag{65}$$

The angles α_{tail} predicted by (65) are shown in figure 11 within parentheses directly below the experimental data of Lang. This comparison, however, should be properly qualified, since the application of the two-dimensional theory tends to overestimate the efficiency, determination of the effective mean chord is crude, and the accuracy of the measured α_{tail} was claimed to be somewhat uncertain. These rather obscure circumstances notwithstanding, it is still of significance to observe that the general trend of the predicted α_{tail} is in fair accordance with the experimental measurements.

In terms of Lighthill's form (56) of the lateral motion, the location of the pitch-axis corresponding to the Z_p and α_p given by (64) assumes the value, by (57),

$$b/l = \tfrac{1}{2}(\sin 7°)/(0{\cdot}104) = 0{\cdot}585, \tag{66}$$

and the corresponding feathering parameter is, by (60),

$$\theta = (0{\cdot}208/0{\cdot}228)(\sec 7°) = 0{\cdot}92. \tag{67}$$

The above value of b/l locates the pitch axis at $\frac{1}{2}(1+0{\cdot}585) = 0{\cdot}793$-chord point from the leading edge, which is well in the favourable range predicted by Lighthill (1970, see particularly his figure 4). The value of feathering parameter $\theta = 0{\cdot}92$ is somewhat higher than the range 0·6 to 0·8 discussed by Lighthill, but it is in the right direction for higher efficiencies. Finally, an interpolation check with figures 8–10 shows that the observed reduced frequency $\sigma = 0{\cdot}228$ is somewhat greater than the σ_m (which is about 0·14 for the $\bar{C}_{T,0}$ at hand), the leading-edge suction at this σ is, nevertheless, still reasonably small,

$$C_S/C_T \simeq 0{\cdot}4.$$

In conclusion, the following comments are perhaps in order about the main features of the tail movement. (i) The estimated reduced frequency $\sigma = 0{\cdot}228$ is large compared with $\sigma_c = 0{\cdot}01$, but lies well in the range in which the leading-edge suction is not large. (ii) The loading parameter $\bar{C}_{T,0}$ ($= 1{\cdot}6 \times 10^{-3}$ as estimated) turns out to be very small, mainly owing to the large amplitude of heaving. (iii) The phase difference $\alpha_p = 263°$ between the pitching (about the mid-chord) and heaving modes falls in the range of σ where α_p is nearly stationary, and is 'safely' away from the region of rapid changes of α_p. (iv) With pitching kept only at a rather small amplitude ($Z_p = 0{\cdot}11$ in this case) but with the correct phase α_p, impressively high efficiency ($\eta \sim 0{\cdot}99$) can be achieved. (v) When the heaving is forcibly made to lead the pitching by 90° in phase, the pitch axis is at about 0·8-chord point, and the feathering ($\theta = 0{\cdot}92$) is nearly accurate. It seems quite conclusive that (i) is the primary condition for selecting the frequency σ in practice.

5. Movements of bird's wing in flapping flight

The present two-dimensional theory can also be used to discuss qualitatively the optimal movement of a bird's wing in flapping flight as most species of migrating birds have wings of high aspect-ratio, and there must be a considerable saving of energy with optimum wing movement. We shall again adopt the strip theory to give a first-order estimate, leaving the effect of finite span as a further refinement. A somewhat superficial difference between fish propulsion and bird flight arises from the need in the latter case of adding to the oscillatory motion the constant angle of attack required for supporting the body weight in air. But this steady component can be accounted for separately; it does not correlate with the oscillatory component in the balance of mean energy.

Take the z-axis to lie along the mean position of the wing span, with the wing stretched from $z = -b$ to b. The wing motion is assumed to have primarily a heaving and a pitching mode, so that, for a wing strip at station z, the up-and-down flapping displacement in the y-direction can be written

$$h = \{\tfrac{1}{2}\xi_0(z) + [\xi_1(z) + j\xi_2(z)]\,x\}\exp(j\omega t) \quad ((x, z) \in S), \tag{68}$$

where S denotes the plane form of the wing, and the amplitude functions ξ_n's generally depend on z, they being real and even functions of z for symmetrical

motions. Ordinarily, bending of the wing is relatively small except possibly near the tip. To fix our ideas, we assume

$$\xi_0(z) = c_0(z - z_c) \quad (0 < z < b), \tag{69}$$

so that $(c_0 z_c)$ gives the amplitude of the vertical displacement of body centroid, which is probably quite small in general. The z-dependence of ξ_1 and ξ_2 can then be discussed qualitatively based on the argument of optimum efficiency.

Suppose for simplicity that the chord is nearly constant along the span, except in the vicinity of the wing tip, so that the reduced frequency σ referred to the local half-chord is almost uniform. To simplify the picture, we further assume that the spanwise distribution of the thrust coefficient C_T is approximately constant, and fixed as required for overcoming the viscous drag. According to the present optimum solution, high efficiencies very close to unity can be achieved if σ is sufficiently greater than σ_c, and if the local $\bar{C}_{T,0} = C_{T,0}/\xi_0^2$ is sufficiently small, a condition which can be satisfied by making the amplitude ξ_0 of flapping large. This high efficiency η implies that C_P will be nearly equal to C_T (since $1 - C_T/C_P = 1 - \eta \ll 1$), and hence also will be almost uniformly distributed along the span. However, since the flapping amplitude $\xi_0(z)$ grows monotonically outwards from $z = z_c$, we have

$$\partial \bar{C}_{T,0}/\partial z = -(2C_{T,0}/\xi_0^3)(d\xi_0/dz) < 0 \quad (z > z_c),$$

so that $\bar{C}_{T,0}$ decreases rapidly towards the wing tip. Figure 6 then indicates that the amplitude ratio $Z_p = (\xi_1^2 + \xi_2^2)^{\frac{1}{2}}/\xi_0$ should increase slightly with z, implying that $(\xi_1^2 + \xi_2^2)^{\frac{1}{2}}$ should increase at least at the same rate as ξ_0 towards the wing tip. Furthermore, figure 7 indicates that the phase advance angle α_p of pitching should also increase with decreasing $\bar{C}_{T,0}$ as z moves towards the wing tip. In this range of σ, α_p is somewhat smaller than 270°. The general picture is then roughly as follows: As the wing flaps up and down, the pitching amplitude increases with the distance outward from the body, reaching a nearly horizontal position at the top and bottom of each stroke. Such a wing movement, according to this simple strip-theory argument, is the most efficient, and leaves behind the least possible vorticity in overcoming a given frictional drag. This crude picture may be further refined by employing a more accurate lifting-line or lifting-surface theory, and by including physiological considerations about limitations of physical structure, muscular power, metabolic rate and other factors. Such a broad study is, however, out of the scope of present considerations.

6. The general optimum shape problem

As soon as the shape function $h(x,t)$ of a flexible plate is allowed to have a higher number of possible modes, with more Fourier coefficients $\beta_0, \beta_1, \beta_2, \ldots, \beta_N (2 < N \leqslant \infty)$ admitted to h (see (2)), the optimum shape problem immediately becomes more involved. To begin with, we note that the degree of complexity of the analysis depends somewhat on the primary, but crucial, step of choosing the independent variable between h and V. If h is taken as the independent

function, having the Fourier expansion (2), the Fourier coefficients of V (see (4)) can be expressed in terms of the β_n's as

$$b_n/U = j\sigma\beta_n + 2\sum_{s=0}^{\infty}(2s+n+1)\beta_{2s+n+1} \quad (n = 0, 1, 2, \ldots). \tag{70}$$

The analysis subsequent to this approach can be developed along a line very much similar to the previous case of two-term expansion discussed in §3, the major step being again the reduction of the singular quadratic form C_E to a non-singular one of a lower order. It turns out that the first non-singular reduced quadratic form of C_E is always of order 2 regardless of the value $N\,(>2)$ to begin with. This is not surprising, since C_E depends on only the first two Fourier coefficients b_0, b_1 of V. This property of C_E also explains the advantages of taking V as the independent function.

It is convenient first to decompose V as

$$V(x,t)\exp(-j\omega t)/U = (c_1+jc_2)\cos\theta + V_\perp(x) \quad (x = \cos\theta), \tag{71a}$$

$$V_\perp(x) = c_0(\tfrac{1}{2}-\cos\theta) + \sum_{n=2}^{\infty}(c_{2n-1}+jc_{2n})\cos n\theta, \tag{71b}$$

in which the c_n's are all real, and the coefficient of the constant term is taken to be purely real as a reference phase. By comparison with (4),

$$b_0/U = c_0, \quad b_1/U = (c_1-c_0)+jc_2, \quad b_n/U = c_{2n-1}+jc_{2n} \quad (n = 2, 3, \ldots), \tag{72}$$

in which the time factors $\exp(j\omega t)$ of the b_n's are omitted as understood. The above representation of V is complete, and is so decomposed that $V_\perp(x)$ is orthogonal to $(1+x)$, i.e. by (12),

$$(V_\perp, 1+\cos\theta) = 0, \tag{73}$$

whence

$$(V,\ 1+\cos\theta) = b_0+b_1 = U\exp(j\omega t)(c_1+jc_2). \tag{74}$$

The plate movement $h(x,t)$ corresponding to the above V can be determined by integration of (3), giving

$$h(x,t) = \exp(-j\sigma x)\left\{\int_0^x \exp(j\sigma\xi)\frac{V(\xi,t)}{U}d\xi + \tfrac{1}{2}(\xi_5+j\xi_6)\exp(j\omega t)\right\} \quad (-1 < x < 1), \tag{75}$$

where $(\xi_5+j\xi_6)$ is a constant of integration, which becomes known once $h(0,t)$ is prescribed. Upon substituting (71) in (75),

$$h(x,t)\exp(-j\omega t) = \frac{c_1+jc_2}{\sigma^2}(1-j\sigma x-\exp(-j\sigma x)) + h_\perp(x) + \tfrac{1}{2}(\xi_5+j\xi_6)\exp(-j\sigma x), \tag{76a}$$

$$h_\perp(x) = \exp(-j\sigma x)\int_0^x \exp(j\sigma\xi)V_\perp(\xi)d\xi. \tag{76b}$$

Again we note that h can admit a progressing wave $\exp[j(\omega t-\sigma x)]$ without affecting V.

The Fourier coefficients β_n's of h can be derived from (76) by making use of the Fourier–Bessel expansion (Watson 1944, p. 22)

$$\exp(\pm j\sigma\cos\theta) = J_0(\sigma) + 2\sum_{n=1}^{\infty}(\pm j)^n J_n(\sigma)\cos n\theta. \tag{77}$$

The first two coefficients are determined as

$$\beta_0\exp(-j\omega t) = 2(c_1+jc_2)\frac{1-J_0(\sigma)}{\sigma^2} + (\xi_1+j\xi_2) + (\xi_5+j\xi_6)J_0(\sigma), \tag{78a}$$

$$\beta_1\exp(-j\omega t) = \frac{c_1+jc_2}{j\sigma}\left[1-\frac{2}{\sigma}J_1(\sigma)\right] + (\xi_3+j\xi_4) - j(\xi_5+j\xi_6)J_1(\sigma), \tag{78b}$$

$$\xi_1+j\xi_2 = \frac{2}{\pi}\int_0^{\pi} h_\perp(x)\,d\theta, \quad \xi_3+j\xi_4 = \frac{2}{\pi}\int_0^{\pi} h_\perp(x)\cos\theta\,d\theta. \tag{78c}$$

Upon substituting (74) and (78) into (6)–(7), we obtain

$$C_E = B(\sigma)(c_1^2+c_2^2), \tag{79}$$

$$C_P = \tilde{P}_{22}(c_1^2+c_2^2) + \sigma\tilde{A}_1c_1 + \sigma\tilde{A}_2c_2, \tag{80a}$$

where

$$\tilde{P}_{22} = (1-\mathscr{F})\left[1-\frac{2}{\sigma}J_1(\sigma)\right] + \frac{2}{\sigma}\mathscr{G}[1-J_0(\sigma)], \tag{80b}$$

$$\begin{aligned}\tilde{A}_1+j\tilde{A}_2 = {}& (\xi_1+j\xi_2)(\mathscr{G}+j\mathscr{F}) - (\xi_3+j\xi_4)[\mathscr{G}-j(1-\mathscr{F})] \\ & + (\xi_5+j\xi_6)[(\mathscr{G}+j\mathscr{F})J_0(\sigma) + (1-\mathscr{F}+j\mathscr{G})J_1(\sigma)].\end{aligned} \tag{80c}$$

The present result (79)–(80) is now seen to be analogous to the previous case of rigid plate, (35)–(37). Proceeding in a similar way, we extremize C_E, with again $C_T = C_{T,0}$ fixed (see (10)), by varying first c_1 and c_2. The variational solution, containing σ, $C_{T,0}$ as well as $(\xi_1, \ldots, \xi_6)$ as a family of parameters, is of the form,

$$c_1 = \lambda\tilde{A}_1, \quad c_2 = \lambda\tilde{A}_2, \tag{81}$$

λ being a Lagrange multiplier. By substituting (81) in (79)–(80)

$$C_E = B(\lambda\tilde{A})^2, \quad C_P = (\tilde{P}_{22}\lambda^2+\sigma\lambda)\tilde{A}^2, \quad \tilde{A}^2 = |\tilde{A}_1+j\tilde{A}_2|^2. \tag{82}$$

Application of condition (10) now yields

$$\tilde{T}_{22}\lambda^2 + \sigma\lambda = \tilde{C}_{T,0}, \tag{83a}$$

where

$$\tilde{T}_{22} = \tilde{P}_{22} - B, \quad \tilde{C}_{T,0} = C_{T,0}/(\tilde{A})^2. \tag{83b}$$

In this case, λ again has two solutions:

$$\left.\begin{matrix}\lambda_1 \\ \lambda_2\end{matrix}\right\} = \frac{\sigma}{2\tilde{T}_{22}}\{-1 \pm (1+\tilde{\Lambda})^{\frac{1}{2}}\}, \quad \tilde{\Lambda} \equiv \frac{4}{\sigma^2}\tilde{T}_{22}\tilde{C}_{T,0}. \tag{84}$$

In comparing this result with (42) of the rigid plate case, we note that the general feature of $\tilde{T}_{22}(\sigma)$ is quite similar to T_{22}, namely, $\tilde{T}_{22}$ vanishes at $\sigma = 0$ and $\sigma = \tilde{\sigma}_0 = 2{\cdot}51$, and

$$\tilde{T}_{22}(\sigma) \gtrless 0 \quad \text{according as} \quad \sigma \gtrless \tilde{\sigma}_0 = 2{\cdot}51. \tag{85}$$

The derivative $d\tilde{T}_{22}/d\sigma$ is found to be appreciably smaller than $dT_{22}/d\sigma$, as is shown in figure 1. From this property it follows that, if the parameter $\tilde{C}_{T,0}$ of

this solution assumes the same value as $\bar{C}_{T,0}$ in the rigid plate case, the rate of increase $d\tilde{\Lambda}/d\sigma$ is slower than $d\Lambda/d\sigma$, and hence the critical reduced frequency $\tilde{\sigma}_c < \sigma_c$, where $\tilde{\Lambda}(\tilde{\sigma}_c, \tilde{C}_{T,0}) = -1$, and σ_c is given by (43). Consequently, λ_1 and λ_2 will be real if $\tilde{\Lambda} \geqslant -1$, or

$$\sigma \geqslant \tilde{\sigma}_c(\tilde{C}_{T,0}) \quad \text{where} \quad \tilde{\Lambda}(\tilde{\sigma}_c, \tilde{C}_{T,0}) = -1. \tag{86}$$

Within this range of σ, λ_1 corresponds to the maximum efficiency,

$$\eta_{\max} = \frac{C_{T,0}}{C_P} = 1 - \frac{C_E}{C_P} = 1 - \frac{B\lambda_1}{\tilde{P}_{22}\lambda_1 + \sigma} \quad (\sigma \geqslant \tilde{\sigma}_c), \tag{87}$$

whereas λ_2 yields the minimum efficiency

$$\eta_{\min} = C_{T,0}/C_{P,\max} = 1 - \frac{B\lambda_2}{\tilde{P}_{22}\lambda_2 + \sigma} \quad (\sigma \geqslant \tilde{\sigma}_c). \tag{88}$$

The present optimum solution, being not yet subjected to the recoil conditions, contains the parameters $\sigma, C_{T,0}, \xi_1, \xi_2, \ldots \xi_6$. When these eight parameters are prescribed, λ_1 is given by (84), c_1 and c_2 by (81), and the optimum profile h is furnished by (76), except the component $h_\perp(x)$ is determinate only up to the first two Fourier coefficients (see (78*c*)). To this end, we note that the Fourier coefficients of $h_\perp(x)$ higher than the second have no influence upon the optimum efficiency. Furthermore, it is of significance to observe that the parameters $\xi_1, \xi_2, \ldots \xi_6$ appear in the solution of $\eta_{\max}$ only through the quantity $\tilde{A}^2$, which is a quadratic form of $\xi_1, \xi_2, \ldots \xi_6$ with frequency-dependent coefficients. Consequently, every point $(\xi_1, \xi_2, \ldots \xi_6)$ on the quadrics $\tilde{A}^2 = \text{const.}$ will yield the same $\eta_{\max}$. This result shows that the optimum solution, as presently posed, can be determined only to a certain degree, but not to the extent to provide a unique $h(x,t)$. The reason for this, as mentioned earlier, is because there appears in this variational problem only a few scalar products involving h and V.

Judging from the known properties of the rigid plate solution, which are quite similar to the present general case, it can be inferred that for fixed σ and $C_{T,0}$, $\eta_{\max}$ will increase with decreasing $\tilde{\Lambda}$, or with increasing $\tilde{A}^2$ (see (84)). Furthermore, $\eta_{\max}$ very close to unity can be attained when $C_{T,0}/(\tilde{A})^2 \ll 1$.

The actual numerical work can be facilitated by first expressing the quadratic form $\tilde{A}^2$ in the canonical form. A possible choice of the new variables is

$$\zeta_1 = \xi_1 - \hat{\xi}_1(\xi_3, \ldots \xi_6), \quad \zeta_2 = \xi_2 - \hat{\xi}_2(\xi_3, \ldots \xi_6), \tag{89a}$$

where $\hat{\xi}_1$ and $\hat{\xi}_2$ are the values of ξ_1 and ξ_2, respectively, which will make $\tilde{A}_1 + j\tilde{A}_2$ and hence also $\tilde{A}^2$ vanish for arbitrary $(\xi_3 \ldots \xi_6)$. Then (80*c*) becomes

$$\tilde{A}_1 + j\tilde{A}_2 = (\mathscr{G} + j\mathscr{F})(\zeta_1 + j\zeta_2), \tag{89b}$$

hence

$$\tilde{A}^2 = (\mathscr{F}^2 + \mathscr{G}^2)(\zeta_1^2 + \zeta_2^2), \tag{89c}$$

this being in the canonical form. Clearly, $\eta_{\max}$ depends on two parameters $[\sigma, C_{T,0}/(\zeta_1^2 + \zeta_2^2)]$, c_1 and c_2 depend on four parameters $(\sigma, C_{T,0}, \zeta_1, \zeta_2)$, whilst β_0 and β_1 depend on $(\sigma, C_{T,0}, \zeta_1, \zeta_2, \xi_3, \xi_4, \ldots \xi_6)$. The above canonical form is not unique. The expression for $\tilde{A}_1 + j\tilde{A}_2$ in (80*c*) indicates several other combinations of new variables. For instance, as another set, one may take

$$\zeta_3 = \xi_3 - \hat{\xi}_3(\xi_1, \xi_2, \xi_5, \xi_6), \quad \zeta_4 = \xi_4 - \hat{\xi}_4(\xi_1, \xi_2, \xi_5, \xi_6), \tag{90a}$$

where $\hat{\xi}_3$ and $\hat{\xi}_4$ are such that $\tilde{A}_1+j\tilde{A}_2$ vanishes at $\xi_3=\hat{\xi}_3$, $\xi_4=\hat{\xi}_4$. Then

$$\tilde{A}_1+j\tilde{A}_2 = -[\mathscr{G}-j(1-\mathscr{F})](\zeta_3+j\zeta_4), \tag{90b}$$

and the corresponding form of $\tilde{A}^2$ is again canonical.

For each of these canonical forms of $\tilde{A}^2$, the calculation of the optimum $\eta_{\max}$ will be entirely parallel to the special case of the rigid plate, although there remain additional free parameters in the determination of the optimum shape. It may be expected that due to the additional degrees of freedom admitted to $h(x,t)$ for this general case, $\eta_{\max}$ will be further improved from the rigid plate value at fixed σ and $C_{T,0}/\xi_{50}^2$, ξ_0 being the heaving amplitude.

Finally, suppose the body recoil conditions (15)–(16) are also to be satisfied, then these two conditions will give four scalar equations relating four more parameters of V, say c_3, c_4, c_5, c_6, to the remaining unknown coefficients. This shows that $h(x,t)$ as given by (76) can be determined to a higher degree, the lack of complete determinateness of the optimum shape remains, nevertheless, an intrinsic feature of the problem.

I am deeply indebted to Professor M. J. Lighthill for interesting and stimulating discussions, and particularly for calling my attention to the significance of leading-edge suction in this problem. My remarks in this paper would have been less complete had I not had the privilege of knowing his important contribution (1970) prior to its publication. I am also grateful to Dr T. G. Lang for discussion on his experiments, and to Professors C. R. De Prima and Duen-pao Wang for their interest in the general problem presented in §6. Assistance provided by Dr Arthur Whitney and Mr Allen Chwang in numerical studies is greatly appreciated. This work was partially sponsored by the National Science Foundation, under Grant GK 10216, and by the Office of Naval Research, under Contract N00014-67-A0094-0012.

REFERENCES

Lang T. G. & Daybell, D. A. 1963 *NAVWEPS Rept.* 8060; *NOTS Tech. Publ.* 3063.

Lighthill, M. J. 1969 *Ann. Rev. Fluid Mech.* **1**, 413.

Lighthill, M. J. 1970 *J. Fluid Mech.* **44**, 265.

Wang, P. K. C. 1966 *IEEE Trans. Automatic Control*, AC **11**, 645.

Watson, G. N. 1944 *A Treatise on the Theory of Bessel Functions* (2nd edn.). Cambridge University Press.

Wu, T. Y. 1971 *J. Fluid Mech.* **46**, 337.